30 Mar 2001, 1:30 pm - 3:30 pm

New Observations and Methods for Modeling Nonlinear Site Response

Ralph J. Archuleta
University of California, Santa Barbara, CA

Daniel Lavallée
University of California, Santa Barbara, CA

Luis Fabián Bonilla
University of California, Santa Barbara, CA

NEW OBSERVATIONS AND METHODS FOR MODELING NONLINEAR SITE RESPONSE

Ralph J. Archuleta
Institute for Crustal Studies
and Department of Geological Sciences
University of California, Santa Barbara, CA 93106

Daniel Lavallée
Institute for Crustal Studies
University of California, Santa Barbara, CA 93106
Luis Fabián Bonilla
Institute for Crustal Studies
and Department of Geological Sciences
University of California, Santa Barbara, CA 93106

ABSTRACT

Observations of nonlinear effect in earthquake strong ground motion include Bonds Corner, 1979 Imperial Valley, CA; Wildlife Refuge accelerogram, 1987 Superstition Hills, CA; and the Kushiro Port station, 1993 Kushiro-Oki, Japan, among others. To understand the nature of these nonlinear effects, we have developed a model of nonlinear soil dynamics that includes nonlinear effects such as anelasticity, hysteretic behavior and cyclic degradation due to pore water pressure. The hysteresis behavior is given by the Generalized Masing rules. This new formulation has a functional representation and it includes the Cundall-Pyke hypothesis and Masing original formulation as special cases. It also provides a mean to quantify anelastic damping as a function of the stress-strain loop. Using the in situ observations from the Garner Valley downhole seismographic array (GVDSA), we have modeled scenarios of ground motions at the surface for this site. The simulations show amplitude reduction as well as the shift of the fundamental frequency to lower frequencies as observed on vertical arrays. The synthetic accelerograms show the development of intermittent behavior—high frequency peaks riding on low frequency carrier—as observed in the acceleration records mentioned above. Comparisons between the nonlinear model predictions and those computed with the equivalent linear model demonstrate that the latter model fails to capture essential manifestations of nonlinear soil response.

INTRODUCTION

While nonlinearity in seismic ground motion is often inferred, there are only few cases where nonlinearity has been directly observed in strong ground motion accelerograms. Moreover predicting strong ground motion time histories requires quantifying the degree of nonlinearity associated with different levels of input motion coupled with characteristics of the site geology. First we will present a new characteristic of accelerograms that we believe is a direct result of nonlinearity in the soil during strong ground shaking. Then to understand the behavior of the soil during strong shaking we have developed a general formulation of hysteresis based on the Masing rules. The generalized Masing rules provide a framework for understanding the nonuniform dilation and translation of stress-strain loops for a material subject to non-periodic stresses; they also provide a means for understanding anelastic damping as function of the stress-strain loops. These new generalized Masing rules are coupled to pore pressure effects by a constitutive equation in the strain space based on the multishear mechanism concept (Towhata and Ishihara, 1985; Iai, 1990a, b). The generalized Masing rules together with the pore pressure are implemented in a nonlinear one-dimensional finite difference method. Numerical modeling of a soil column produces the characteristics associated with nonlinear soil response such as a shift of the fundamental frequency to longer periods, damping, and shear modulus reduction. It also produces the intermittent behavior of the soil in exacerbating the duration, intermittent peaks in acceleration and a shift of low-frequency energy to higher frequency that produces a complex amplitude spectrum not found in the usual equivalent linear formulation. We use this new formulation of soil hysteresis behavior to examine case histories of known nonlinear soil response as well as to investigate the role of critical parameters in affecting the soil response.

NONLINEAR EFFECTS IN ACCELEROGRAMS

Since the seminal work of Seed and Idriss (1967), several direct and indirect observations of nonlinear effects in observed seismograms have been reported (see Beresnev and Wen, 1997; and Archuleta *et al.*, 1999 for comprehensive reviews). The paucity of direct observations is due to the complex and intermittent nature of these nonlinear effects. An exhaustive list is outside the scope of this proposal, but some typical signatures of nonlinearity have been reported in the literature, with direct consequences on man-made structures.

Among the clearest examples of nonlinear response are the Port Island borehole records of the 1995 Hyogo-ken Nambu earthquake (Iwasaki and Tai, 1996). In the acceleration records there is a clear change in the high-frequency waveforms of acceleration with less obvious changes in the low-frequency velocity and displacement time histories. While not as direct an observation as from borehole recordings, nonlinear response is generally associated with accelerograms that show a pronounced change in frequency content that occurs during or immediately after strong shaking. A classic example of such behavior is the response at Treasure Island (a soft soil site) during the 1989 Loma Prieta earthquake. Fortunately there was an accelerogram recorded on rock about two kilometers away at Yerba Buena Island for comparison (Fig. 1).

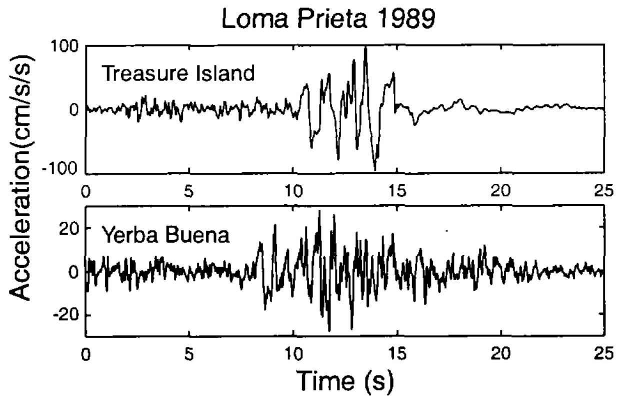

Fig. 1. Horizontal accelerograms (north-south) from the 1989 Loma Prieta earthquake recorded at two sites that are within 2.5 kilometers of each other.

Other than borehole observations of strong shaking or in the serendipity situation where accelerograms are recorded at rock and soil sites close to each other, nonlinearity of the soil must be inferred by indirect methods. A basic approach is to compare the transfer function for weak and strong ground motion recorded at the same site. The principal observation one expects for nonlinear response is a shift of the fundamental frequency of the transfer function to longer period. A major difficulty with this approach is finding a reference site. Using data from the 1994 Northridge earthquake Field *et al.* (1996) compared the average amplification of strong and weak shaking for a class of soil sites with that of a few rock sites to infer widespread nonlinear soil response at frequencies between 1.0 and 4.0 Hz. In a study of the 1989 Loma Prieta earthquake Idriss (1990) compared peak accelerations on rock sites compared to soil sites for the same event to infer nonlinear response. Borehole data provide an excellent baseline for such studies (Satoh *et al.* 1995, 1997; Wen *et al.*, 1994). However the downgoing waves (those reflected from the free surface and other pronounced changes in impedance) can produce specious peaks in the transfer function that might be interpreted as a shift in the fundamental frequency (Steidl *et al.*, 1996).

In some strong motion accelerograms there is a characteristic waveform that we have associated with nonlinear response (Archuleta, 1998). One of the most obvious examples of this waveform is clearly observed in the Port Kushiro surface acceleration time history (Fig. 2) resulting from the 1993 Kushiro-oki earthquake (Iai *et al.*, 1995). Thorough analysis of this surface record by Iai *et al.* (1995) leaves no doubt that the spiky waveform is the result of nonlinear response of the soil. Porcella (1980) cited as examples of atypical accelerograms: Bonds Corner, 15 October 1979 Imperial Valley earthquake (Fig. 3); Cerro Prieto accelerogram, 9 June 1980 northern Mexico earthquake; and four recordings at the left abutment of Long Valley Dam from four M>6 earthquakes in May 1980 near Mammoth Lakes.

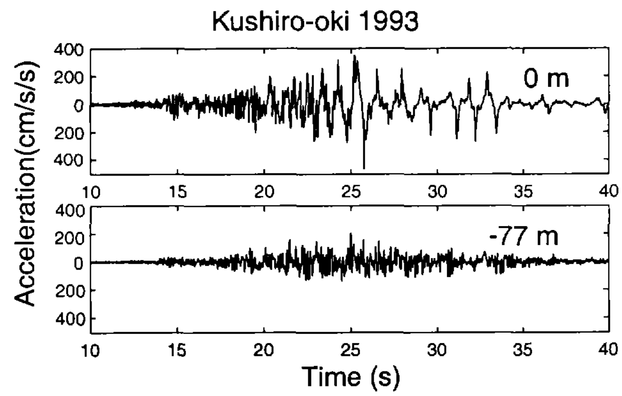

Fig. 2. Surface (0 m) and borehole (-77 m) acceleration time histories for a dense sand deposit during the 1993 Kushiro-oki earthquake. Note the spiky repetitive waveform that dominates the surface starting at about 25 seconds.

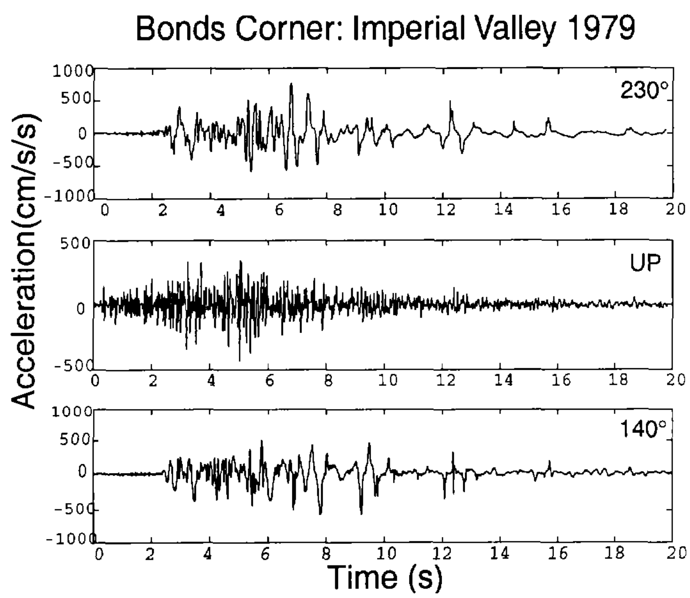

Fig. 3. Accelerograms for Bonds Corner recorded during the 1979 Imperial Valley earthquake. Note the spiky acceleration starting around 6 s and coming after the main S waves.

This characteristic waveform is also present in the Wildlife Refuge recordings of the 1987 Superstition Hills earthquake (Holzer *et al.*, 1989; Zeghal and Elgamal, 1994), the fault normal Takatori accelerogram of the 1995 Hyogo-ken Nanbu earthquake (Kamae *et al.*, 1998) and the 1994 Northridge accelerogram recorded at Sylmar Converter Station in the Van Norman Dam Complex (Bardet and Davis, 1996). This characteristic waveform is a direct consequence of nonlinear soil response at Kushiro Port (Iai *et al.*, 1995) and the Wildlife Refuge (Zeghal and Elgamal, 1994). The Wildlife Refuge recorded the M 6.2 Elmore Ranch earthquake only 12 hours before the M 6.7 Superstition Hills event. Theanalysis of these records from these two earthquakes clearly suggest that the spiky behavior is due to nonlinearity in the soil response. The analysis of the records at the Wildlife Refuge array Zeghal and Elgamal, (1994) associated the spikes in the accelerationtime history with episodes of dilatancy in corresponding pore pressure measurements that were simultaneously recorded (Holzer *et al.*, 1989). For both Kushiro Port and the Wildlife Refuge the investigators have pinpointed the nonlinear dilatant behavior of the soil as the probable cause of the spiky accelerations. The Wildlife Refuge site experienced liquefaction at the surface, but the Kushiro Port site did not.

This manifestation of nonlinearity, multiple occurrences of similar shaped acceleration spikes, is significantly different from previous observations in that the nonlinearity does not diminish the high frequency nature of the accelerograms or necessarily reduce the peak acceleration. In the case of Kushiro-Oki (Fig. 2) and Bond's Corner (Fig. 3) the peak acceleration is a peak of one of these characteristic waveforms. The other critical effect on the accelerograms is that the nonlinearity extends the duration of strong shaking as opposed to the commonly held view that nonlinearity will reduce the duration of strong shaking, e.g., Treasure Island (Fig. 1). This nonlinear effect creates a time history that has, late in the record, high accelerations that are a site effect, not a source effect. Models of soil nonlinearity must account for such effects as observed at sites experiencing strong shaking.

INTRODUCTION TO GENERALIZED MASING RULES

In principle, the issue of the origin of nonlinearity can be addressed through an appropriate formulation of nonlinear soil dynamics near the earth surface, followed by the solution of the resulting equations (usually obtained via numerical integration techniques). To study and understand the phenomenology of nonlinear soil response to earthquake, we have developed a numerical model that captures the essential physics of nonlinearity in soil. The model includes anelasticity, hysteretic behavior and pore water pressure. It is based on the assumption of one-dimensional vertical propagation of the three components of earthquake motion. This is a common and reasonable assumption when there is no indication of potential effects due to basin or other geologic structure. The soil profile is represented as a series of horizontal layers. The model assumes continuum mechanics and implements a finite-difference based numerical integration of the 1-D shear wave equation of motion with appropriate boundary and initial conditions:

$$\rho \frac{\partial^2 u}{\partial t^2} = \frac{\partial \tau}{\partial z} \qquad (1)$$

Here $u(z,t)$ denotes the displacement field perpendicular to the vertical axis at position z and time t; ρ is the unstrained density of the material, and $\tau(z,t)$ is the shear stress. The stress-strain relationship of the soil is described by a hyperbolic model, given by the following equation:

$$\tau = \frac{G_{\max}\gamma}{1+\left|\frac{G_{\max}}{\tau_{\max}}\gamma\right|} + \eta\frac{\partial\gamma}{\partial t} \qquad (2)$$

where $\gamma(z,t) = \partial u(z,t)/\partial z$ denotes the shear strain, $G_{\max}$ is the maximum shear modulus at low strain; $\tau_{\max}$ is the maximum stress that the material can support in the initial state, and η is the viscosity factor. The first term on the right hand side of Eq. (2) corresponds to the anelastic properties, while the second term corresponds to energy dissipation by viscosity.

Several hysteresis models have been developed and discussed in the literature (e.g., Pyke, 1979, Li and Liao, 1993; McCall, 1994; Muravskii and Frydman, 1998; and Xu *et al.*, 1998). In this paper, the hysteretic behavior is implemented with the generalized Masing rules (Archuleta *et al.*, 1999, 2000). This formulation of hysteresis is based on the original Masing rules. The generalized Masing rules provide a framework for understanding the nonuniform dilation and translation of stress-strain loops for a material subject to non-periodic stresses (or strains). This new hysteresis formulation has several interesting features. It has a functional representation and it includes the Cundall-Pyke hypothesis (Pyke, 1979) and Masing original formulation (see Kramer, 1996) as special cases. In its most elementary implementation, the generalized Masing rule is even simpler than the Masing and extended Masing rules (Kramer, 1996). The model depends only on one free parameter γ_f named the fiducial point. This parameter controls the size of the loop in the stress-strain space and therefore can be related to the amount of energy dissipated through the nonlinear property of the material. In other words, the generalized Masing rules provide a mean to introduce the effect of the damping ratio into nonlinear modeling independently of the other soil parameters (on this specific issue see the discussion in Ishihara, 1996). The relationship between the anelastic damping of a stress-strain loop and the fiducial point for cyclic loadings has been derived in Archuleta *et al.*, 1999.

In the Generalized Masing rules , the initial loading is given by the backbone curve $F_{bb}(\gamma)$ equals to the right side of Eq. (2). For the subsequent loadings and unloadings, the strain-stress relationship is given by the following tranformation:

$$\frac{\tau - \tau^{(i)}}{c_H} = F_{bb}\left(\frac{\gamma - \gamma^{(i)}}{c_H}\right) \qquad (3)$$

until the path prescribed by Eq. (3) crossed the backbone curve (Eq. 2) in the stress-strain space. Then the current loading or unloadings return to the backbone curve until the next turning point where Eq. (3) applied again and the rules are iterated. The coordinate $(\gamma^{(i)}, \tau^{(i)})$ corresponds to the i^{th} (and previous) reversal points in the strain-stress space. In Masing's original formulation, the hysteresis scale factor c_H is equal to 2.0. In the generalized Masing rules, c_H is a function of physical properties of the material and of γ_f (Archuleta *et al.*, 1999, 2000). In the stress-strain space, γ_f controls the intersection between the path given by Eq. (3) and the backbone curve. The Generalized Masing rules can be summarized by the following relation:

$$\tau(\gamma)=\begin{cases} F_{bb}(\gamma) & \gamma<\gamma^{(1)}, t<t^{(1)} \\ c_H^{(n)}F_{bb}\left(\dfrac{\gamma-\gamma^{(n)}}{c_H^{(n)}}\right)+\tau^{(n)} & |\gamma|\le|\gamma_f|, t\ge t^{(1)} \\ F_{bb}(Sign(\frac{d\gamma}{dt})\gamma) & |\gamma|\ge|\gamma_f|, t\ge t^{(1)} \end{cases} \quad (4)$$

where $t^{(1)}$ is the time corresponding to the first turning point and $\tau^{(n)}$ is given by the following relation:

$$\tau^{(n)}=\sum_{i=2}^{n}c_H^{(i-1)}F_{bb}\left(\frac{\gamma^{(i)}-\gamma^{(i-1)}}{c_H^{(i-1)}}\right)+F_{bb}\left(\gamma^{(1)}\right) \quad (5)$$

where $\gamma^{(n)}$ correspondsto the turning point at the n^{th} unloading or reloading (the index n is even at reloading and odd when unloading). The time derivative in Eq. (4) is estimated at any time between the n^{th} and the $(n+1)^{th}$ turning point. The function *Sign* returns 1 when its argument is positive, 0 when the argument is 0, and -1 when its argument is negative. The third rule in Eq. (4) does not apply for $\gamma_f \to \infty$ and is optional for $\gamma_f=\gamma^{(1)}$. The first rule in the right hand side of Eq. (5) corresponds to the first loading path. The second rule governs the hysteresis behavior of successive unloading and reloading paths until $|\gamma|$ exceeds $|\gamma_f|$. The term $\tau^{(n)}$, given by Eq. (5), is determined by the contribution of the previous turning point. When $|\gamma|>|\gamma_f|$, the third rule in Eq. (4) specifies that the stress-strain path follows the backbone equation. Memory of all previous turning points is erased each time the strain-stress path returns to the backbone curve.

When the backbone curve is given by the hyperbolic model (Eq. 2), the expression for $c_H^{(n)}$ is given by the following relation:

$$c_H^{(n)}=\frac{\left(F_{bb}(Sign(\frac{d\gamma}{dt})|\gamma_f|)-\tau^{(n)}\right)\left|Sign(\frac{d\gamma}{dt})|\gamma_f|-\gamma^{(n)}\right|}{\left(Sign(\frac{d\gamma}{dt})|\gamma_f|-\gamma^{(n)}\right)\tau_{max}+\left(\tau^{(n)}-F_{bb}(Sign(\frac{d\gamma}{dt})|\gamma_f|)\right)\gamma_{ref}} \quad (6)$$

where the referencestrain $\gamma_{ref}=\tau_{max}/G_{max}$. Note that, in general, the parameter $c_H^{(n)}$ will have a different value for different unloadings or reloadings. It is convenient to bound the parameter γ_f by the following relationship $|\gamma^{(1)}|\le|\gamma_f|<\infty$, where $\gamma^{(1)}$ corresponds to the first turning point and the upper bound corresponds to the Cundall-Pyke hypothesis (Pyke, 1979). For the ground motion calculations discussed in this paper, $\gamma_f=\gamma^{(1)}$ with implementation of the third rule in Eq. (4).

PORE PRESSURE MODEL

In order to take into account the pore pressure development during cyclic loads, we need to couple the hysteresis model with an effective stress model. The chosen constitutive equation is the strain space multishear mechanism. This formulation was first implemented by Towhata and Ishihara (1985) to simulate pore pressure generation in sands under cyclic loading and undrained conditions, and further developed by Iai *et al.* (1990a, b) to take into account the cyclic mobility and dilatancy of sands. The methodology has the following advantages: (1) it is relatively easy to implement, it has few parameters and they can be obtained from simple laboratory tests with pore pressure generation; (2) since the theory is a plane strain condition, it can be developed to study problems in two dimensions, e.g. embankments, quay walls, among others; (3) the pore pressure built up depends on the cumulative shear work done during the shaking, so that the correlation between laboratory data and predicted ground motion is simple.

MODELING OF STRONG GROUND MOTION AT GVDA

The last 30 years have seen a period of continuous study of nonlinear wave propagation in granular and cohesive soils. Although there have been significant advances in both theory and numerical techniques, the equivalent linear method (Schnabel *et al*, 1972) is the most commonly used method in earthquake engineering studies. One may speculate that the popularity of the equivalent linear method is due to the small number of parameters needed and its simplicity. Another asset of the model, especially meaningful for computers of the previous generations, was the short amount of computing time required to perform the calculation. Some comparisons between the equivalent linear and nonlinear modeling show similar results at least for strains less than 0.1% (EPRI, 1993; Ishihara, 1996). However for larger strains, the equivalent linear method overestimates the peak ground acceleration and overdamps the high frequencies of the computed ground motion (Yoshida and Iai, 1998). This is precisely the range where saturated cohesionless materials develop strong pore pressure and large deformations that can only be studied by the integration of the wave equation, step by step, in the time domain with an appropriate nonlinear rheology (e.g. Towhata and Ishihara, 1985; Iai *et al*, 1990a, b; Zienckewicz *et al*, 1999). In this section we pursue the comparison between a full nonlinear formulation of soil dynamics and the equivalent linear method.

The nonlinear model of soil, with and without pore pressure, has been used to generate scenario of strong ground motion at the Garner Valley Downhole Array (GVDA; for more details see Archuleta *et al*, 1999, other examples are presented in Archuleta *et al*, 1999; 2000). The input motion used is the acceleration time history at GL-55 m from the M 6.1 Joshua Tree earthquake of April 23, 1992. Knowing the velocity profile of the material above the sensor, we compute the response for an impulse at the sensor depth. This impulse response allows us to compute those waves that are travelling downward at the sensor. These waves are removed from the input time history. Thus the computed incident motion is used as an elastic boundary condition (Joyner and Chen, 1975). The computed input ground acceleration is then scaled to peak ground acceleration (PGA) values of 25 gals and propagated to the surface using the equivalent linear method and the nonlinear model.

The computed surface waveforms are illustrated in Fig. 4. The predicted peak ground accelerations are similar for the equivalent linear model and the nonlinear model without pore pressure. Acceleration time histories computed with the nonlinear model including pore pressure generates the maximum peak acceleration. The frequency content, however, varies significantly among the model predictions. The accelerogram computed with the equivalent linear method produces a signal depleted of high frequencies. Note how even the beginning of the waveform computed by the equivalent linear method differs from the nonlinear computations in the lack of high frequencies and lower amplitude. In addition, the duration of the strong motion is smaller when compared to the nonlinear results. This is even more important when the pore pressure is taken into account. The computed accelerogram produces intermittent spikes with peaks up to 0.2 g late in the record in the time interval of 20 to 25 s. Similar manifestations of nonlinearity have been also detected in Figs. 1, 2 and 3. Although the nonlinear computation with no pore pressure provides lower acceleration, the duration of the strong motion is still significant as well as its high frequency. This effect cannot be only attributed to the inclusion of pore pressure.

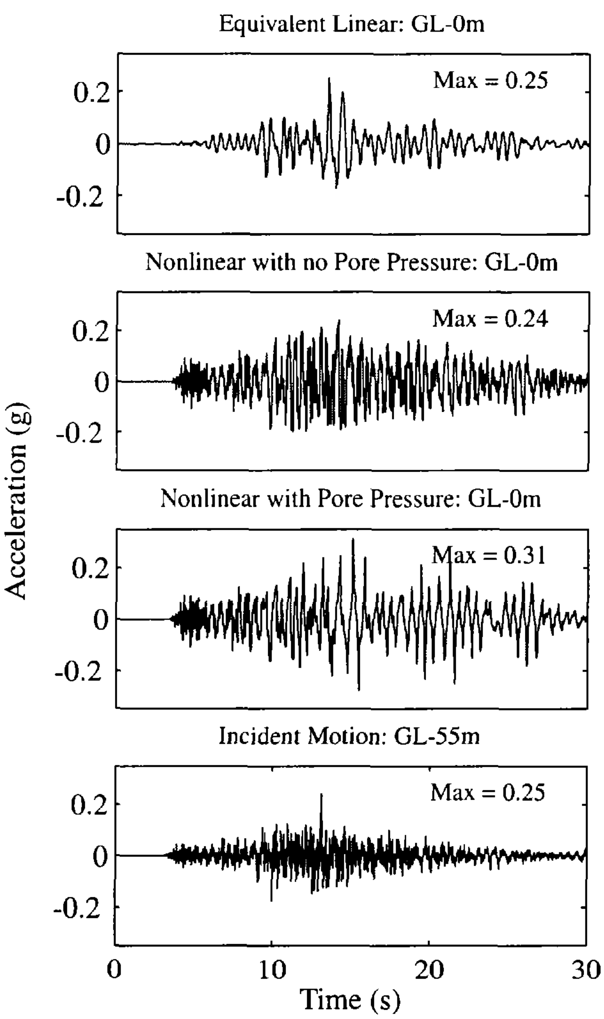

Fig. 4. Acceleration time histories computed using the equivalent linear and nonlinear methods. The input motion is given at the bottom. Note that the nonlinear computations show larger duration of the strong motion and more high frequency content. Inclusion of pore pressure produces intermittence as well as large accelerations late in the record.

CONCLUSION

There is a new direct observation of nonlinearity in soils: late manifestation of quasi repetitive high-frequency spikes in the acceleration time history. For instance, this nonlinear effect can be detected in Bond's Corner accelerogram and the Kushiro Port accelerogram. To understand the nature of this nonlinearity, we have coupled a new hysteresis model, the generalized Masing rules, with a multiple shear mechanism rheology (Towhata and Ishihara, 1985; Iai *et al.*, 1990a, b). The numerical solutions show an increase in the spectral response for frequencies larger than the fundamental as well as a splitting of the frequency peaks. The generalized Masing rules coupled with pore pressure can reproduce the high-frequency acceleration spikes of large large-amplitude as observed in recorded strong ground signals. This phenomenon increases the duration of the strong shaking and in some circumstance produces the maximum acceleration. The increase in spectral amplitudes and increased duration of strong shaking are not normally associated with nonlinear effects although different soil models have suggested this effect (e.g., Yu *et al.*, 1992). Comparisons of the nonlinear model predictions with those computed with the equivalent linear model for the identical physical situation indicate that the equivalent linear model is incapable of explaining much of the behavior that is observed in nonlinear soil response. Furthermore, the computing time required to perform a nonlinear calculation has significantly decreased with the advent of a new generation of powerful computers. The simulations reported in the previous section can be computed on a personal computer. Taking advantage of this technological advances, the study and the modeling of earthquake strong ground motion can now be achieved with a full inclusion of nonlinear soil dynamics.

ACKNOWLEDGMENTS

We thank Dr. Susumu Iai for providing the Kushiro accelerograms as well as his help on implementing his constitutive model for nonlinear response. This work was supported by the U. S. Nuclear Regulatory Commission, NRC-04-96-046 and the French Institute de Protection et de Surete Nucleaire, #4060-00001217. D. Lavallée acknowledges support from the NSF grant EAR-9972987 This paper is ICS contribution No. 0368-109EQ.

REFERENCES

Archuleta, R. J. [1998). Direct observation of nonlinear soil response in accelerationtime histories, Seism. Res. Lett. pp. 69, 149.

Archuleta, R.J., L.F. Bonilla, and D. Lavallée [1999]. Nonlinear Site Response Using Generalized Masing Rules Coupled with Pore Pressure, Proc. of the OECD-NRC Workshop on Engineering Characterization of Seismic Input, Brookhaven National Laboratory, NY, 32.

Archuleta, R.J., L. F., Bonilla, and D. Lavallée [2000]. Nonlinearity in observed and computed accelerograms. Proc. of the 12th World Conference on Earthquake Engineering, published by Aston Koedyk Ltd. Paper reference number 0338.

Bardet, J. P., and C. A. Davis [1996]. Engineering Observations on Ground Motion at the Van Norman Complex after the 1994 Northridge Earthquake, Bull. Seism. Soc. Am., 86, pp. S333-S349.

Beresnev, I. A., and K. L. Wen [1997]. Nonlinear site response-A reality?, Bull. Seism. Soc. Am., 86, pp. 1964-1978.

EPRI [993]. *Guidelines for Determining Design Basis Ground Motions*, Vol. 2: Appendices for Ground Motion Estimation.

Field, E. H., Johnson, P. A., Beresnev, I. A and Zeng, Y. [1997]. Nonlinear ground-motion amplification by sediments during the 1994 Northridge earthquake, Nature 390, pp. 599-602.

Holzer, T. L., Youd, T. L. and Hanks, T. C. [1989]. Dynamics of liquefaction during the 1987 Superstition Hills, California, earthquake, Science 244, pp. 56-59.

Iai, S., Y. Matsunaga and T. Kamoka, [1990a], Strain space plasticity model for cyclic mobility, Report of Port and Harbour Research Institute, 29, No 4, pp. 27-55.

Iai, S., Y. Matsunaga and T. Kamoka, [1990b], Parameter identification for a cyclic mobility model, Report of Port and Harbour Research Institute, 29, No 4, pp. 57-83.

Iai, S., Morita, T., Kameoka, T., Matsunaga, Y. and Abiko, K. [1995], Response of a dense sand deposit during 1993 Kushiro-Oki Earthquake, Soils and Foundations 35, pp. 115-131.

Idriss, I., M. [1990], Response of soft soil sites during earthquakes, in J. M. Dunca, ed., Proceedings, H. Bolton Seed memorial Symposium, BiTech Publishers, Vancouver, BC, Vol. 2, pp. 273-289.

Ishihara, K., [1996], *Soil Behaviour in Earthquake Geotechnics*, Clarenton Press, Oxford.

Iwasaki, Y. and Tai, M. [1996]. Strong motion records at Kobe Port Island, Special Issue of Soils and Foundations, January 1996, pp. 29-40.

Joyner, W.B. and A.T.F. Chen [1975]. Calculation of Nonlinear Ground Response in Earthquakes, Bull. Seism. Soc. Am. 65, pp. 1315-1336.

Kamae, K., Irikura, K. and Pitarka, A. [1998]. A technique for simulating strong ground motion using hybrid Green's functions, Bull. Seism. Soc. Am. 88, pp. 357-367.

Kramer, S. L. [1996], *Geotechnical Earthquake Engineering*, Prentice Hall, New Jersey.

Li, X. and Z. Liao, [1993]. Dynamic skeleton curve of soil stress-strain relation under irregular cyclic loading Earthquake research in China, 7, pp. 469-477.

McCall, K. R., [1994]. Theoretical study of nonlinear elastic wave, J. Geophys. Res., 99, pp. 2591-2600.

Muravskii, G., and S. Frydman [1998]. Site response analysis using a non-linear hysteretic model. Soil dynamics and Earthquake Engineering, 17, pp. 227-238.

Pyke, R. [1979]. Nonlinear soil model for irregular cyclic loadings, J. of the Geotech. Eng. Div. 105 (6), pp. 715-726.

Porcella, R. L. [1980]. Atypical accelerograms recorded during recent earthquakes, Seismic Engineering Program Report. May-August: 1980, Geological Survey Circular 854-B, 1-7.

Satoh, T., Sato, T. and Kawase, H. [1995]. Nonlinear behavior of soil sediments identified by using borehole records observed at the Ashigara Valley, Japan, Bull. Seism. Soc. Am. 85, pp. 1821-1834.

Satoh, T., Horike, M., Takeuchi, Y., Uetake, T. and Suzuki, H. [1997]. Nonlinear behavior of scoria soil sediments evaluated from borehole records in Eastern Shizuoka Prefecture, Japan, Earthquake Eng. Struct. Dyn. 26, pp. 781-795.

Seed, H. B., and I. M. Idriss, [1967]. Analysis of Soil Liquefaction: Nigata earthquake, J. of Soil Mechanics and Foundations Divisions, ASCE, Vol. 93, No. SM3.

Steidl, J. H., Tumarkin, A. G. and Archuleta, R. J. [1996]. What is a reference site?, Bull. Seism. Soc. Am.. 86, pp. 1733-1748.

Towhata, I. and K. Ishihara [1985]. Modeling Soil Behavior Under Principal Axes Rotation, Fifth Int. Conf. on Numerical Methods in Geomechanics, Nagoya, pp. 523-530.

Wen, K., Beresnev, I. and Yeh, Y. T. [1994]. Nonlinear soil amplification inferred from downhole strong seismic motion data, Geophys. Res. Lett. 21, pp. 2625-2628.

Yoshida, N. and S. Iai [1998]. Nonlinear Site Response and its Evaluation and Prediction, Proce. of the Sec. Int. Symp. on the Effects of Surface Geology on Seismic Motion, Vol. 1, edited by K. Irikura, K. Kudo H. Okada and T. Sasatani, A.A. Balkema: Netherlands, pp. 71-90.

Yu, G., Anderson, J. G. and Siddharthan, R. [1992], On the characteristics of nonlinear soil response, Bull. Seism. Soc. Am.. 83, pp. 218-244.

Xu, H., S. M. Day, and J. B. Minster. [1998]. Model for nonlinear wave propagation derived from rock hysteresis measurements. J. Geophys. Res., 103, 29915-29929.

Zeghal, M. and Elgamal, A-W. [1994]. Analysis of site liquefaction using earthquake records, J. Geotech. Eng. 120, pp. 996-1017.

Zienkiewicz, O.C., A.H. Chan, M. Pastor, B.A. Schrefler, and T. Shiomi [1999]. *Computational Geomechanics, with Special Reference to Earthquake Engineering* John Wiley & Sons, New York.